

Joint Association and Resource Allocation for Multi-Hop Integrated Access and Backhaul (IAB) Network

Byungju Lim, Ju-Hyung Lee, Jae-Hong Kwon, Ki-Hun Kim, Jong-Man Lee, Hyun Park, Young-Seok Ha, Young-Jin Han, and Young-Chai Ko

Abstract—Integrated access and backhaul (IAB) network is envisioned as a novel network architecture for increasing the network capacity and coverage. To facilitate the IAB network, the appropriate methods of wireless link association and resource management are required. In this paper, we investigate the joint optimization problem of association and resource allocation in terms of subchannel and power for IAB network. In particular, we handle the association and resource allocation problems for wireless backhaul and access links considering multi-hop backhauling. Since the optimization problem for IAB network is formulated as a mixed integer non-linear programming (MINLP), we divide it into three subproblems for association, subchannel allocation, and power allocation, respectively, and these subproblems are solved alternatively to obtain a local optimal solution. For the association problem, we adopt the Lagrangian duality approach to configure the backhaul and access links and successive convex approximation (SCA) approach is used to solve the subchannel and power allocation problems efficiently. Simulation results demonstrate that the proposed algorithm achieves better performance than single-hop (SH) backhauling based network and enhances the capacity and coverage by configuring the multi-hop (MH) backhauling.

Index Terms—Association, integrated access and backhaul, power allocation, subchannel allocation, wireless backhaul.

I. INTRODUCTION

THE fifth generation (5G) and beyond 5G networks are envisioned to increase the capacity by 1000 fold for the rapid growth of data traffic. To cope with exponentially increasing traffic demands, massive multiple-input multiple-output (MIMO) and mmWave technologies are considered

as major capacity enhancing techniques, which exploits the benefits of spatial reuse and wide bandwidth [1]. However, to take the advantage of mmWave communications, we need to overcome several challenges such as high propagation loss and high sensitivity to blockages, which makes the network coverage limited [2], [3]. For seamless coverage in mmWave communications, network densification where the low-power small cell base stations (SBSs) are densely deployed has been regarded as a possible approach [4], [5].

Heterogeneous network (HetNet) where SBSs are overlaid within macro BS (MBS) requires a backhaul connection between the core networks and SBSs [6]. Tradition approach for backhaul connection is wired backhauling which provides high speed and reliable communications. However, implementing the optical fiber backhaul link for the large-scale deployment of SBSs is infeasible due to the prohibitive cost. In this respect, mmWave based wireless backhauling has been considered as an alternative that can be scalable in the network densification and provide the gigabit per second (Gbps) data rates [7]. Wireless backhauling effectively supports ever-increasing backhaul traffic demands while it has benefits in both hardware costs and deployment difficulties [8]. Furthermore, using the beamforming technique, spatial reuse can be exploited in the wireless backhauling such that it can provide the immunity against inter-cell interference [7]. However, the extra radio resources and infrastructure are essential for implementing the mmWave based wireless backhaul.

In-band wireless backhaul, referred to as self-backhauling, utilizes the same resources and infrastructure for the access link [9]. Accordingly, it does not require the extra spectrum for backhaul link and the existing infrastructure can be used to serve backhaul as well as access link. With the advantages of in-band wireless backhaul, 3GPP introduces the integrated access and backhaul (IAB) which has been standardized in 5G NR [10]. According to [10], the main characteristics of IAB are the integration of wireless access and backhaul links, the use of mmWave spectrum, and the plug-and-play installation of IAB-nodes facilitated by wireless backhaul. Unlike the long term evolution (LTE) relay that has the limited functionalities of single-hop relaying and fixed resource partitioning, IAB network is capable of supporting multi-hop backhauling and enabling resource management between access and backhaul links. Meanwhile, the new interference results from access and backhaul links due to the sharing resources, which should be mitigated to ensure the quality-of-service (QoS) of each user. Therefore, the joint design of RAN and backhaul network is challenging in the IAB network [11].

Manuscript received September 13, 2022; approved for publication, September 19, 2022. This paper is specially handled by EIC and Division Editor with the help of three anonymous reviewers in a fast manner.

This work was supported by Korea Research Institute for Defense Technology (KRIT)-Grant funded by Defense Acquisition Program Administration (DAPA) (KRIT-CT-22-036)

Part of this work was presented to IEEE ICTC, Oct, 2021.

B. Lim is with the Department of Electronic Engineering, Pukyong National University, Busan, 48513, South Korea. email: limbj@pknu.ac.kr.

J.-H. Lee is with Ming Hsieh Department of Electrical and Computer Engineering, University of Southern California, Los Angeles, CA 90007, USA. email: juhyung.lee@usc.edu.

J.-H. Kwon, and Y.-C. Ko are with the School of Electrical Engineering, Korea University, Seoul 02841, South Korea. email: {hugokwon, koyc}@korea.ac.kr.

K.-H. Kim, J.-M. Lee, and H. Park are with Hanwha Systems, South Korea. email: {kihun19.kim, jongman0319.lee, h82.park}@hanwha.com.

Y.-S. Ha and Y.-J. Han are with Korea Research Institute for Defense Technology Planning and Advancement (KRIT), South Korea. email: {ace1002, gksdudwls2}@krit.re.kr.

Y.-C. Ko is the corresponding author.

Digital Object Identifier: 10.23919/JCN.2022.000041

Creative Commons Attribution-NonCommercial (CC BY-NC).

This is an Open Access article distributed under the terms of Creative Commons Attribution Non-Commercial License (<http://creativecommons.org/licenses/by-nc/3.0>) which permits unrestricted non-commercial use, distribution, and reproduction in any medium, provided that the original work is properly cited.

Multi-hop (MH) backhauling, one of the advantages of IAB technology, is a promising solution to enhance the network throughput and coverage [12], [13]. By exploiting the spatial reuse in IAB with MH backhauling, the blockage issue and the interference management in IAB network need to be efficiently addressed. Hence, the design of MH backhauling including topology management, route selection, and dynamic resource allocation between backhaul and access links, is important and challenging issues in the IAB network [14]. However, designing the MH-IAB network may be difficult due to the flexibility of deployment and configuration. Thus, efficient network design in-between access and backhaul links for MH-IAB is demanded while considering the interference caused by in-band wireless backhaul and blockage issues. Motivated by these emerging IAB architecture, several research activities have investigated the design of IAB network for both backhaul and access links such as resource management [15], [16] and finding optimal routing and user association in the IAB network [17], [18].

A. Related Work

Several works investigated the performance of IAB network based on stochastic geometry [11], [19]. In particular, authors in [11], [19] analyzed the effects of bandwidth partition between access and backhaul links and presented an optimal bandwidth partition ratio for access and backhaul links. In [20]–[23], the resource allocation for HetNet has been investigated. The resource management for time and frequency has been designed for maximizing the sum throughput under the existence of cross-tier interference in [20], [21]. Authors in [22] investigated the spectrum allocation problem between access and backhaul links for in-band and out-band full-duplex based SBSs. Besides in [23], the joint association and bandwidth allocation problem for wireless backhaul studied for two-tier HetNets. However, these works only consider SH backhauling where all the SBSs are directly connected to MBS, such that the advantages of IAB network are not fully exploited.

MH backhauling has been recently investigated in [17], [24], [25] to guarantee the coverage and the line-of-sight (LoS) condition for backhaul. In [24], the resource allocation for backhaul was studied to configure the MH backhauling under fixed backhaul traffic. Besides in [25], the framework of MH network for the resource management was addressed based on matching game theory. Moreover, optimal strategies for backhaul link selection were investigated in [17] to configure MH backhauling where high quality first (HQF) selects the link with the highest SNR as a backhaul and wired first (WF) selects a direct link to MBS with the highest SNR above a threshold. Despite of the studies for MH backhauling, all of these works do not consider the user traffics which significantly affect the overall network performance and the optimal backhaul link configuration. Thus, it cannot provide the adaptive backhaul configuration under different traffic requirements of users.

B. Main Contribution

As aforementioned, the MH backhauling is a promising solution for the coverage and the blockage issues in IAB network. It is vital to efficiently design the MH backhauling and allocate resources between access and backhaul links. To the best of our knowledge, the joint design of resource allocation and association for the MH backhauling while considering the traffics of users has not been investigated. In this paper, for MH-IAB network, we jointly optimize the association and resource allocation with respect to subchannel and power considering the dynamic user traffic demands. Our proposed algorithm presents the optimized association of backhaul and access links and improves the network throughput by allocating the subchannel and power for each link. Our contributions are summarized as follows:

- 1) We propose the joint resource allocation and association optimization to enhance the network throughput while guaranteeing the quality of service (QoS) of users. In particular, we consider inter-cell interference and cross-tier interference caused by shared resources between SBSs and MBS.
- 2) To solve the optimization problem, we propose the three stages based iterative algorithm. Firstly, the MH backhauling based optimal association is proposed using the Lagrangian duality approach. We observe that the blockage issue, which is a major obstacle for the coverage, is circumvented by configuring the MH backhauling and it achieves a higher LoS probability for backhaul links.
- 3) In the second and third stages, the subchannel and power allocation algorithms are proposed, respectively. We transform them into a sequence of convex problems based on SCA, which are the lower bound of the original problem, and the low complexity algorithms are proposed to solve these subproblems. Particularly, the mixed integer programming of subchannel allocation is addressed by employing the continuous relaxation and penalty function. As a result, some simulation results confirm that the proposed algorithm provides better throughput and coverage performance than SH backhauling.

The rest of this paper is organized as follows. Section II presents the system and channel model for IAB network and the joint optimization problem is formulated in Section III. In Section IV, we solve the joint optimization problem by dividing it into three subproblems and the complexity of proposed algorithm is analyzed. The simulation results are discussed in Section V to verify the performance of proposed scheme and finally conclusion is provided in Section VI.

II. SYSTEM MODEL

A. IAB Network Scenario

Consider a two-tier HetNet where B SBSs are distributed in a macrocell with MBS at its center. We assume that MBS and SBS are equipped with N_m and N_s antenna arrays, respectively, and K user equipments (UEs) equipped with N_u

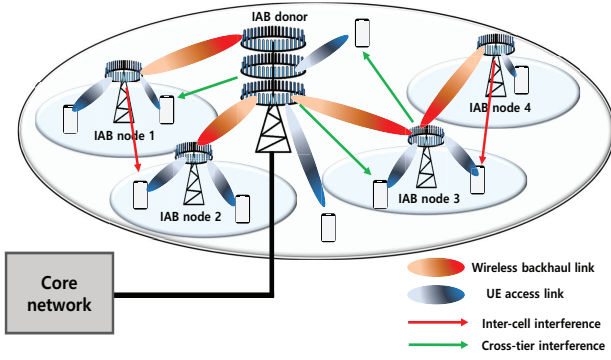


Fig. 1. Multi-hop IAB based two-tier heterogeneous network.

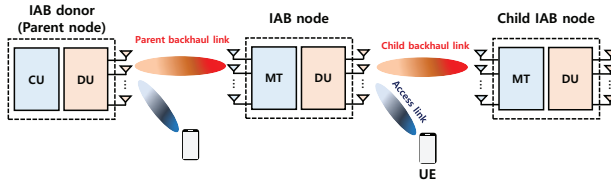


Fig. 2. Basic architecture of multi-hop IAB network.

antenna arrays are served by MBS or SBS. It is also assumed that MBS is connected to core networks with high speed optical fiber and provides wireless backhaul connectivity for SBSs that are connected to the core networks through MBS. Note that wireless backhaul can be supported between SBSs since IAB can provide MH wireless backhauling as illustrated in Fig. 1 [10]. Throughout this paper, IAB-donor is referred to as MBS and SBS indicates an IAB-node since SBS acts as an IAB-node.

The IAB architecture is based on 5G NR functionality split where radio link control (RLC) and packet data convergence protocol (PDCP) is split. Thus, IAB-donor consists of a central unit (CU) and a distributed unit (DU) where DU includes RLC, medium access control (MAC), and physical layer (PHY) protocols [26]. Moreover, IAB-node consists of a DU and a mobile terminal (MT) to simultaneously support both of backhaul and access links. In particular, as shown in Fig. 2, DU of IAB-node is used to serve the child IAB-node and its associated UE, while MT is used to maintain the wireless backhaul connection to the parent DU which might be IAB-donor or IAB-node [14]. IAB network can enable SH and MH wireless backhauling owing to its flexible network topology [27], while C-RAN only supports SH backhauling, which is the key difference between C-RAN and IAB network.¹ In particular, IAB-donor always acts as the parent node of all the IAB-nodes. On the other hand, both IAB-donor and IAB-node can serve as the parent node in MH backhauling. It should

¹It is noted that conventional C-RAN is composed of the baseband unit (BBU) and the remote radio heads (RRHs) where RRH performs the radio frequency (RF) and some signal processing functionalities [28]. Hence, RRH is responsible for transmitting and receiving the RF signals whereas IAB-node is responsible for network configuration and scheduling of both access and backhaul links. In addition, RRH is directly connected to BBU over wired or wireless medium, which is referred to as single-hop (SH) backhauling.

TABLE I
NOTATION OF VARIABLES.

Notation	Definition
B	Number of SBSs
K	Number of Users
M	Number of subchannels
N_m	Number of antennas for MBS
N_s	Number of antennas for SBS
N_u	Number of antennas for UE
L	Number of NLoS paths
$\mathcal{B}, \mathcal{B}_0$	Sets of SBSs and all BSs including MBS
\mathcal{K}	Set of UEs
\mathcal{I}	Set of SBSs and UEs
\mathcal{M}	Set of subchannels
R_i^{th}	Minimum data rate requirement of the i th UE
P_b^{max}	Maximum transmit power at the b th BS
$\beta_{\text{LoS}}, \beta_{\text{NLoS}}$	Path loss exponent for LoS and NLoS paths
$\sigma_{\text{LoS}}, \sigma_{\text{NLoS}}$	Standard deviation of shadow fading for LoS and NLoS paths
$\gamma_{b,i,m}$	SINR of the i th node from the b th BS over the m th subchannel
$\mathbf{H}_{b,i,m}$	Channel matrix for the i th node from the b th BS over the m th subchannel
$\mathbf{v}_{b,i,m}, \mathbf{w}_{b,i,m}$	Precoding and combining vector for the i th node from the b th BS over the m th subchannel.
$x_{b,i,m}$	Subchannel allocation variable for the i th node from the b th BS over the m th subchannel
$y_{b,i}$	Association variable for the i th node from the b th BS over the m th subchannel
$P_{b,m}$	Power allocation variable for the b th BS over the m th subchannel

be noted that all the backhaul and access links use mmWave spectrum.

Throughout this paper, we refer to the link between UE and IAB-DU as access link, the link between the IAB-MT and its parent node as parent backhaul link, and the link between the IAB-DU and its child IAB-MT as child backhaul link. For the mathematical convenience, $\mathcal{B}_0 = \{0\} \cup \mathcal{B}$ denotes the set of all BSs, in which the index 0 represents MBS while $\mathcal{B} = \{1, 2, \dots, B\}$ represents the set of SBSs (e.g., IAB-nodes). Let $\mathcal{I} = \mathcal{B} \cup \mathcal{K}$ denote the set of all SBSs and UEs where $\mathcal{K} = \{B+1, B+2, \dots, B+K\}$ is the set of UEs. The set of subchannels denoted as $\mathcal{M} = \{1, 2, \dots, M\}$ comprises with M subchannels. The notation used throughout this paper is summarized in Table I.

B. Channel Model

1) *LoS and NLoS Channel*: We consider a well-known frequency-dependent path loss (PL) model, namely the close-in free space reference distance PL (CI-PL) model [29], which is given by

$$\text{PL}(\beta, d) [\text{dB}] = a + 10\beta \log_{10} d_{[\text{m}]} + \chi, \quad (1)$$

where $a = 20 \log_{10} (4\pi f_c / c)$ is the free space path loss with 1 m reference distance, d [m] is the distance from Tx to Rx, β is the path loss exponent, and χ is the log-normal shadow fading. Note that f_c and c are the carrier frequency and the speed of light, respectively.

Since the path loss exponent depends on whether there is a LoS path or not, the CI-PL models for LoS and NLoS are separately defined as $\text{PL}_{\text{LoS}}(d) = \text{PL}(\beta_{\text{LoS}}, d)$ and

$PL_{\text{NLoS}}(d) = PL(\beta_{\text{NLoS}}, d)$, respectively. Furthermore, the small-scale fading channels for LoS and NLoS paths are given respectively as

$$\begin{aligned} \mathbf{H}_{b,i,m}^{\text{LoS}} &= \sqrt{N_t N_r} \alpha_{b,i,m}^{\text{LoS}} \mathbf{a}(\theta_{b,i}) \mathbf{a}^H(\phi_{b,i}), \\ \mathbf{H}_{b,i,m}^{\text{NLoS}} &= \sqrt{\frac{N_t N_r}{L}} \sum_{l=1}^L \alpha_{b,i,m,l}^{\text{NLoS}} \mathbf{a}(\theta_{b,i,l}) \mathbf{a}^H(\phi_{b,i,l}), \end{aligned} \quad (2)$$

where $\alpha_{b,i}^{\text{LoS}}, \alpha_{b,i}^{\text{NLoS}} \sim CN(0, 1)$, are the channel gain for LoS and NLoS, respectively, $\theta_{b,i}$ and $\phi_{b,i}$ are the angle of departure (AoD) and angle of arrival (AoA) from the b th BS to the i th node, respectively, L is the number of NLoS paths, and N_t and N_r denote the number of Tx and Rx antenna arrays, respectively. Since both MBS and SBS are equipped with uniform linear array (ULA) configuration, the array response vector of the ULA is defined as

$$\mathbf{a}(\theta) = \frac{1}{\sqrt{N}} \left[1, e^{j\frac{2\pi}{\lambda} d_a \sin \theta}, \dots, e^{j\frac{2\pi}{\lambda} (N-1) d_a \sin \theta} \right]^T, \quad (3)$$

where N , θ , λ and d_a are the size of antenna array, the angle of arrival (or departure), the wavelength, and the antenna spacing, respectively. Thus, the channel matrix of the b th BS to the i th node for the m th subchannel is described as

$$\mathbf{H}_{b,i,m} = U_{b,i} PL_{\text{LoS}}^{-\frac{1}{2}}(d_{b,i}) \mathbf{H}_{b,i,m}^{\text{LoS}} + PL_{\text{NLoS}}^{-\frac{1}{2}}(d_{b,i}) \mathbf{H}_{b,i,m}^{\text{NLoS}}, \quad (4)$$

where $U_{b,i}$ is a Bernoulli random variable with LoS probability $P_{\text{LoS}}(d_{b,i})$ and $d_{b,i}$ is the distance between the b th BS and the i th node.

2) *LoS Probability*: For each backhaul and access link, we consider the LoS probability model in [30]. In our IAB network scenario, the following three LoS probability cases are considered:

i) LoS probability for backhaul link :

$$P_{\text{LoS}}^{\text{BH}}(d) = \min\left(\frac{18}{d}, 1\right) \left(1 - e^{-d/72}\right) + e^{-d/72}. \quad (5)$$

ii) LoS probability for access link from MBS to UE :

$$P_{\text{LoS}}^{\text{MBS-UE}}(d) = \min\left(\frac{18}{d}, 1\right) \left(1 - e^{-d/63}\right) + e^{-d/63}. \quad (6)$$

iii) LoS probability for access link from SBS to UE :

$$P_{\text{LoS}}^{\text{SBS-UE}}(d) = 0.5 - \min(0.5, 5e^{-156/d}) + \min(0.5, 5e^{-d/30}). \quad (7)$$

Based on the LoS probability model in (5)–(7), the existence of LoS path for each link is determined. For the backhaul link, we adopt the cell site planning correction factor which can improve the LoS probability of backhaul by finding an optimal place among the candidate SBS sites [30].

C. Signal Model

IAB-node is assumed to be operated in half-duplex mode, which is referred to as out-of-band full duplex (OBFDF) [31]. In other words, the resources for parent backhaul link, child backhaul link, and access link are orthogonally allocated in frequency domain. Note that each subchannel can be used for backhaul or access link in a IAB-node, and it can be reused in different IAB-nodes.

While the self-interference can be neglected due to the half-duplex mode [32], the cross-tier interference and the inter-cell interference should be considered in-between SBSs and the two types of interference considered in the IAB network scenario are illustrated in Fig. 1. Hence, the received signal of the i th node from MBS, which is indexed by 0, over the m th subchannel is expressed as

$$\begin{aligned} r_{0,i,m} &= \sqrt{P_{0,m}} \mathbf{w}_{0,i,m}^H \mathbf{H}_{0,i,m} \mathbf{v}_{0,i,m} s_{0,i,m} \\ &+ \underbrace{\sum_{b' \in \mathcal{B} \setminus \{i\}} \sum_{i' \in \mathcal{B} \setminus \{b', i\}} \sqrt{P_{b',m}} \mathbf{w}_{0,i,m}^H \mathbf{H}_{b',i,m} \mathbf{v}_{b',i',m} s_{b',i',m}}_{\text{Cross-tier interference by backhaul link between SBSs}} \\ &+ \underbrace{\sum_{b' \in \mathcal{B} \setminus \{i\}} \sum_{i' \in \mathcal{K} \setminus \{i\}} \sqrt{P_{b',m}} \mathbf{w}_{0,i,m}^H \mathbf{H}_{b',i,m} \mathbf{v}_{b',i',m} s_{b',i',m}}_{\text{Cross-tier interference by access link in small cell}} \\ &+ \mathbf{w}_{0,i,m}^H \mathbf{n}, \quad \forall i \in \mathcal{I}, m \in \mathcal{M}, \end{aligned} \quad (8)$$

where $s_{b,i,m}$ is the transmitted signal from the b th BS to the i th node on the m th subchannel with $E[|s_{b,i,m}|^2] = 1$, \mathbf{n} is the additive white gaussian noise (AWGN) with zero mean and covariance matrix, $\sigma_n^2 \mathbf{I}$, and $P_{b,m}$ is the allocated power at the b th BS over the m th subchannel. Note that $\mathbf{H}_{b,i,m}$ has the size of $N_s \times N_t$ for $i \in \mathcal{B}$ and $N_u \times N_t$ for $i \in \mathcal{K}$, in which $N_t = N_m$ for $b = 0$ and $N_t = N_s$ for $b \in \mathcal{B}$.

Likewise, the received signal of the i th node from the b th BS on the m th subchannel is expressed as

$$\begin{aligned} r_{b,i,m} &= \sqrt{P_{b,m}} \mathbf{w}_{b,i,m}^H \mathbf{H}_{b,i,m} \mathbf{v}_{b,i,m} s_{b,i,m} \\ &+ \underbrace{\sum_{i' \in \mathcal{I} \setminus \{b\}} \sqrt{P_{0,m}} \mathbf{w}_{b,i,m}^H \mathbf{H}_{0,i,m} \mathbf{v}_{0,i',m} s_{0,i',m}}_{\text{Cross-tier interference}} \\ &+ \underbrace{\sum_{b' \in \mathcal{B} \setminus \{b,i\}} \sum_{i' \in \mathcal{I} \setminus \{b,b',i\}} \sqrt{P_{b',m}} \mathbf{w}_{b,i,m}^H \mathbf{H}_{b',i,m} \mathbf{v}_{b',i',m} s_{b',i',m}}_{\text{Inter-cell interference}} \\ &+ \mathbf{w}_{b,i,m}^H \mathbf{n}, \quad \forall b \in \mathcal{B}, i \in \mathcal{I} \setminus \{b\}. \end{aligned} \quad (9)$$

We note that in (8) and (9), the cross-tier interference and the inter-cell interference can be neglected if the subchannels are orthogonally allocated between all the wireless links.

Let $x_{b,i,m}$ denotes the subchannel allocation variable for the i th node served by the b th BS over the m th subchannel. Then, the signal-to-interference-plus-noise ratio (SINR) is expressed by

$$\begin{aligned} \gamma_{b,i,m}(\mathbf{x}, \mathbf{P}) &= \frac{\alpha_{b,i,m} P_{b,m}}{\sum_{b' \in \mathcal{B}_0 \setminus \{b,i\}} \sum_{i' \in \mathcal{I} \setminus \{b,b',i\}} x_{b',i',m} \alpha_{b',i',m} P_{b',m} + \sigma_n^2}, \end{aligned} \quad (10)$$

where $\alpha_{b,i,m} = |\mathbf{w}_{b,i,m}^H \mathbf{H}_{b,i,m} \mathbf{v}_{b,i,m}|^2$ and $\alpha_{b,b',i,i',m} = |\mathbf{w}_{b,i,m}^H \mathbf{H}_{b',i,m} \mathbf{v}_{b',i',m}|^2$. Here, σ_n^2 is the noise power, and \mathbf{x} and \mathbf{P} are the vector whose elements are $x_{b,i,m}$ and $P_{b,m}$, respectively. Note that the interference occurs when other links use the same m th subchannel, i.e., $x_{b',i',m} = 1$, and interference does not exist, otherwise. Thus, the achievable rate of the

i th node from the b th BS on the m th subchannel in bits per second (bps) is given by

$$R_{b,i,m} = W \log_2(1 + \gamma_{b,i,m}), \quad (11)$$

where W is the bandwidth per subchannel.

III. PROBLEM FORMULATION FOR MULTI-HOP IAB NETWORK

In this section, we jointly formulate the problem of association optimization (AO), subchannel allocation (SA) and power allocation (PA) to maximize the sum rate of UEs for MH-IAB network. Let $y_{b,i}$ denote the association variable where $y_{b,i} = 1$ indicates that the i th node is associated with the b th BS and $y_{b,i} = 0$, otherwise. For MH-IAB network scenario, the optimization problem can be formulated as

$$\begin{aligned}
 (\mathbf{P1}) \quad & \max_{\mathbf{y}, \mathbf{x}, \mathbf{P}} \sum_{b \in \mathcal{B}_0} \sum_{i \in \mathcal{K}} \sum_{m \in \mathcal{M}} y_{b,i} x_{b,i,m} R_{b,i,m} \\
 \text{s.t. } C_1 : & \sum_{b \in \mathcal{B}_0} \sum_{m \in \mathcal{M}} y_{b,i} x_{b,i,m} R_{b,i,m} \geq R_i^{\text{th}}, \quad \forall i \in \mathcal{K}, \\
 C_2 : & \sum_{b' \in \mathcal{B}_0} \sum_{m \in \mathcal{M}} y_{b',b} x_{b',b,m} R_{b',b,m} \\
 & \geq \sum_{i \in \mathcal{I}} \sum_{m \in \mathcal{M}} y_{b,i} x_{b,i,m} R_{b,i,m}, \quad \forall b \in \mathcal{B}, \\
 C_3 : & \sum_{i \in \mathcal{I}} x_{b,i,m} \leq 1, \quad \forall b \in \mathcal{B}_0, m \in \mathcal{M}, \\
 C_4 : & \sum_{i \in \mathcal{I}} x_{b,i,m} + \sum_{b' \in \mathcal{B}_0} x_{b',b,m} \leq 1, \quad \forall b \in \mathcal{B}, m \in \mathcal{M}, \\
 C_5 : & \sum_{b \in \mathcal{B}_0} y_{b,i} = 1, \quad \forall i \in \mathcal{I}, \\
 C_6 : & \sum_{b \in \mathcal{B}} y_{0,b} \geq 1, \\
 C_7 : & y_{b,b'} + y_{b',b} \leq 1, \quad \forall b, b' \in \mathcal{B}_0, \\
 C_8 : & \sum_{m \in \mathcal{M}} P_{b,m} \leq P_b^{\text{max}}, \quad \forall b \in \mathcal{B}_0, \\
 C_9 : & P_{b,m} \geq 0, \quad \forall b \in \mathcal{B}_0, m \in \mathcal{M}, \\
 C_{10} : & y_{b,i} \in \{0, 1\}, \quad \forall b \in \mathcal{B}_0, i \in \mathcal{I}, \\
 C_{11} : & x_{b,i,m} \in \{0, 1\}, \quad \forall b \in \mathcal{B}_0, i \in \mathcal{I}, m \in \mathcal{M},
 \end{aligned} \quad (12)$$

where \mathbf{y} is the vector whose elements are $y_{b,i}$, R_i^{th} is the minimum data rate requirement of the i th UE, and P_b^{max} is the maximum transmit power at the b th BS. The constraint C_1 in (12) represents the QoS requirement for each UE which implies that the dynamic user traffic demands can be satisfied. In C_2 , the data rate of parent backhaul link must be no less than the sum rate of all the access and child backhaul links served by the b th BS. For the constraints related to subchannel, C_3 indicates that each subchannel is allocated to at most one child link (i.e., access or child backhaul link) served by the b th BS, while C_4 represents the half-duplex mode of IAB-node. C_5 ensures that each node is associated with only one BS. Since MBS is only connected to the core networks, at least one IAB-node should be connected to MBS as described in C_6 . Also, C_7 ensures that all the backhaul links are directional. C_8

and C_9 denote the transmit power constraint for each BS and the non-negative transmit power, respectively. Finally, C_{10} and C_{11} indicate that both association and SA variables are binary. Note that without loss of generality, $y_{b,b} = 0$ and $x_{b,b,m} = 0$ are assumed for $b \in \mathcal{B}_0$ since the same transceiver cannot be connected.

Due to binary and continuous variables, (12) is regarded as a mixed integer non-linear programming (MINLP) which is a non-convex and NP-hard problem in general. To solve it, an exhaustive search is required but it is infeasible in practice due to the prohibitive complexity. Several algorithms such as Branch-and-bound can be used to obtain the optimal solution of MINLP problem. However, its complexity for the worst case is as high as an exhaustive search [33]. Therefore, we propose the suboptimal algorithm with low complexity by decomposing the original problem into three sub-problems.

IV. JOINT ASSOCIATION OPTIMIZATION AND RESOURCE ALLOCATION FOR MULTI-HOP IAB NETWORK

To address the non-convex problem in (12), we propose an alternating optimization algorithm. By decoupling the original problem into subproblems and iteratively updating solutions from each subproblem, the original problem can be efficiently solved. In the following subsections, we present the three subproblems for each AO, SA, and PA, and then introduce an alternating algorithm to solve these three subproblems.

A. Association Optimization for Backhaul and Access Links

For given SA variable \mathbf{x} and PA variable \mathbf{P} , (12) can be transformed into the association problem given as

$$(\mathbf{P2}) \quad \max_{\mathbf{y}} \sum_{b \in \mathcal{B}_0} \sum_{i \in \mathcal{K}} y_{b,i} \hat{R}_{b,i} \quad \text{s.t. } C_1, C_2, C_5, C_6, C_7, C_{10}, \quad (13)$$

where $\hat{R}_{b,i} = \sum_{m \in \mathcal{M}} x_{b,i,m} R_{b,i,m}$. However, (13) is still non-convex problem due to the binary constraint C_{10} . To make the problem more tractable, we relax $y_{b,i}$ as a continuous real variable with the range of $[0, 1]$, where the relaxation provides a zero-duality gap [34]. In that case, $y_{b,i}$ can be regarded as a timing sharing factor which is the fraction of time when the i th node is associated with the b th BS. By relaxing the binary variable into the continuous variable, (13) is a linear programming which can be solved using dual problem due to a zero duality gap. The Lagrangian function of (13) can be defined as

$$\begin{aligned}
 L(\mathbf{y}, \boldsymbol{\lambda}, \boldsymbol{\mu}, \nu) = & \sum_{b \in \mathcal{B}_0} \sum_{i \in \mathcal{K}} y_{b,i} \hat{R}_{b,i} \\
 & + \sum_{i \in \mathcal{K}} \lambda_i \left(\sum_{b \in \mathcal{B}_0} y_{b,i} \hat{R}_{b,i} - R_i^{\text{th}} \right) \\
 & + \sum_{b \in \mathcal{B}} \mu_b \left(\sum_{b' \in \mathcal{B}_0} y_{b',b} \hat{R}_{b',b} - \sum_{i \in \mathcal{I}} y_{b,i} \hat{R}_{b,i} \right) \\
 & + \nu \left(\sum_{b \in \mathcal{B}} y_{0,b} - 1 \right), \quad (14)
 \end{aligned}$$

where $\lambda = [\lambda_{B+1}, \dots, \lambda_{B+K}]^T$, $\mu = [\mu_1, \dots, \mu_B]^T$, and ν are the dual variables for the constraints C_1 , C_2 , and C_6 , respectively. Then, the Lagrangian dual problem of (13) can be formulated as

$$\min_{\lambda, \mu, \nu} g(\lambda, \mu, \nu), \text{ s.t } \lambda, \mu, \nu \geq 0. \quad (15)$$

In (15), the dual function $g(\lambda, \mu, \nu)$ can be obtained as

$$g(\lambda, \mu, \nu) = \max_{\mathbf{y}} L(\mathbf{y}, \lambda, \mu, \nu) \\ \text{s.t } C_5, C_7, 0 \leq y_{b,i} \leq 1, \forall b \in \mathcal{B}_0, i \in \mathcal{I}. \quad (16)$$

The Lagrangian dual problem can be solved by decomposing it into inner and outer problems. We first solve the inner problem in (16) to obtain the optimal $y_{b,i}$ for given dual variables and the dual variables are updated at the outer problem in (15). As a result, the inner and outer problems can be iteratively solved until convergence.

For the inner problem, the Lagrangian function can be rewritten as

$$L(\mathbf{y}, \lambda, \mu, \nu) = \sum_{b \in \mathcal{B}_0} \sum_{i \in \mathcal{I}} X_{b,i} y_{b,i}, \quad (17)$$

where

$$X_{b,i} = \begin{cases} (1 + \lambda_i) \hat{R}_{0,i}, & \text{for } b = 0, i \in \mathcal{K} \\ (1 + \lambda_i - \mu_b) \hat{R}_{b,i}, & \text{for } b \in \mathcal{B}, i \in \mathcal{K} \\ \mu_i \hat{R}_{0,i} + \nu, & \text{for } b = 0, i \in \mathcal{B} \\ (\mu_i - \mu_b) \hat{R}_{b,i}, & \text{for } b, i \in \mathcal{B}. \end{cases} \quad (18)$$

Since the i th node needs to select only one BS as in the constraint C_5 , the optimal solution of (16) can be obtained as

$$y_{b,i} = \begin{cases} 1, & b^* = \arg \max_b X_{b,i} \forall i \in \mathcal{I} \\ 0, & \text{otherwise.} \end{cases} \quad (19)$$

Since $X_{b',b} = (\mu_{b'} - \mu_b) \hat{R}_{b',b}$ and $X_{b,b'} = (\mu_b - \mu_{b'}) \hat{R}_{b,b'}$ have a different sign, both $y_{b,b'}$ and $y_{b',b}$ cannot be 1 at the same time which makes the solution in (19) satisfy the constraint C_7 .

To update the dual variables at the outer problem, we adopt the subgradient method given as [35]

$$\lambda_i^{(t+1)} = \left[\lambda_i^{(t)} - \delta_1^{(t)} \left(\sum_{b \in \mathcal{B}_0} y_{b,i} \hat{R}_{b,i} - R_i^{th} \right) \right]^+, \quad (20)$$

$$\mu_b^{(t+1)} = \left[\mu_b^{(t)} - \delta_2^{(t)} \left(\sum_{b' \in \mathcal{B}_0} y_{b',b} \hat{R}_{b',b} - \sum_{i \in \mathcal{I}} y_{b,i} \hat{R}_{b,i} \right) \right]^+, \quad (21)$$

$$\nu^{(t+1)} = \left[\nu^{(t)} - \delta_3^{(t)} \left(\sum_{b \in \mathcal{B}} y_{0,b} - 1 \right) \right]^+, \quad (22)$$

where $[x]^+ = \max(x, 0)$ and $\delta_1^{(t)}$, $\delta_2^{(t)}$, and $\delta_3^{(t)}$ are the positive step sizes at the t th iteration². When using the appropriate step size, the subgradient method guarantees to converge to

²The step size is typically chosen as the constant or square summable but not summable that satisfies $\sum_{k=1}^{\infty} \delta^{(k)^2} < \infty$ and $\sum_{k=1}^{\infty} \delta^{(k)} = \infty$. One example is $\delta^{(t)} = a/(b+t)$ where $a > 0$ and $b \geq 0$ [35].

Algorithm 1 Lagrangian-based AO algorithm

- 1: Initialize T_{\max} , dual variables λ, μ, ν and feasible $x_{b,i,m}$ and $P_{b,m}$
 - 2: Set $t = 0$
 - 3: **repeat**
 - 4: Obtain the association policy $y_{b,i}^*$ as in (19)
 - 5: Update $\lambda^{(t+1)}$, $\mu^{(t+1)}$, and $\nu^{(t+1)}$ as in (20)–(22)
 - 6: Set $t = t + 1$
 - 7: **until** convergence or $t = T_{\max}$
-

the optimal solution since the dual problem is always convex problem.

Based on the solutions of (19)–(22), we propose an iterative algorithm to obtain the association of backhaul and access links. Setting up the maximum iteration number T_{\max} , the proposed algorithm is iteratively continued until convergence or $t = T_{\max}$. In each iteration, the optimal association result is obtained for given dual variables, and dual variables are updated using the subgradient method. Therefore, the algorithm of link association can be summarized as in Algorithm 1.

B. Subchannel Allocation

In this subsection, we optimize SA given AO variable \mathbf{y} and PA variable \mathbf{P} . The subproblem for SA can be written as

$$(\mathbf{P3}) \max_{\mathbf{x}} \sum_{b \in \mathcal{B}_0} \sum_{i \in \mathcal{K}} \sum_{m \in \mathcal{M}} y_{b,i} x_{b,i,m} R_{b,i,m} \\ \text{s.t } C_1, C_2, C_3, C_4, C_{11}. \quad (23)$$

Note that (23) is a non-convex problem due to the binary constraint C_{11} and the non-convex function of $x_{b,i,m} R_{b,i,m}$, which is generally difficult to solve. To facilitate the management of IAB network, the constraints of C_1 and C_2 should be guaranteed for the issues of backhaul bottleneck and QoS requirements. Thus, the algorithm needs to be carefully selected to address those constraints. To handle the non-convexity and satisfy the constraints of (23), we adopt a low complexity iterative algorithm based on successive convex approximation (SCA) that approximates the non-convex problem to a sequence of convex problem. It is known that SCA method guarantees the convergence to a local optimum [36].

First, we need to approximate the non-convex function $x_{b,i,m} R_{b,i,m}$ with the following inequality that is based on first order Taylor series [37].

$$\nu \ln\left(1 + \frac{1}{z}\right) \geq \left(2 - \frac{\bar{\nu}}{\nu}\right) \bar{\nu} \ln\left(1 + \frac{1}{\bar{z}}\right) + \frac{\bar{\nu}}{\bar{z} + 1} \left(1 - \frac{z}{\bar{z}}\right). \quad (24)$$

By substituting $\nu = x_{b,i,m}$, $\bar{\nu} = x_{b,i,m}^{(t)}$, $z = 1/\gamma_{b,i,m}(\mathbf{x}, \mathbf{P})$, and $\bar{z} = 1/\gamma_{b,i,m}(\mathbf{x}^{(t)}, \mathbf{P})$ into (24) for given the obtained SA variable at the t th iteration, denoted by $\mathbf{x}^{(t)}$, we approximate the function $x_{b,i,m} R_{b,i,m}$, and then obtain its lower bound as (25). It is obvious that $\bar{R}_{b,i,m}(\mathbf{x}^{(t)})$ in (25) is a concave function with respect to $x_{b,i,m}$.

Proposition 1: The approximation of (25) provides a tight lower bound.

Proof: Due to the inequality in (24), $x_{b,i,m} R_{b,i,m} \geq \bar{R}_{b,i,m}(\mathbf{x}^{(t)})$ holds as in (25). Note that its equality holds for $\mathbf{x} = \mathbf{x}^{(t)}$ which shows the tightness of the lower bound.

$$\begin{aligned}
x_{b,i,m} R_{b,i,m} &\geq \bar{R}_{b,i,m}(\mathbf{x}^{(t)}) \\
&= \frac{x_{b,i,m}^{(t)}}{\ln 2} \left(2 - \frac{x_{b,i,m}^{(t)}}{x_{b,i,m}} \right) \log_2 \left(1 + \frac{\alpha_{b,i,m} P_{b,m}}{\sum_{b' \in \mathcal{B}_0 \setminus \{b\}} \sum_{i' \in \mathcal{K} \setminus \{b\}} x_{b',i',m} P_{b',m} \alpha_{b,b',i,i',m} + \sigma^2} \right) \\
&\quad + \frac{\alpha_{b,i,m} P_{b,m} x_{b,i,m}^{(t)} / \ln 2}{\alpha_{b,i,m} P_{b,m} + \sum_{b' \in \mathcal{B}_0 \setminus \{b\}} \sum_{i' \in \mathcal{K} \setminus \{b\}} x_{b',i',m}^{(t)} P_{b',m} \alpha_{b,b',i,i',m} + \sigma^2} \left(1 - \frac{\sum_{b' \in \mathcal{B}_0 \setminus \{b\}} \sum_{i' \in \mathcal{K} \setminus \{b\}} x_{b',i',m} P_{b',m} \alpha_{b,b',i,i',m} + \sigma^2}{\sum_{b' \in \mathcal{B}_0 \setminus \{b\}} \sum_{i' \in \mathcal{K} \setminus \{b\}} x_{b',i',m}^{(t)} P_{b',m} \alpha_{b,b',i,i',m} + \sigma^2} \right).
\end{aligned} \tag{25}$$

Using the approximated concave function $\bar{R}_{b,i,m}(\mathbf{x}^{(t)})$, (23) can be reformulated as

$$\begin{aligned}
\text{(P3-1)} \quad &\max_{\mathbf{x}} \sum_{b \in \mathcal{B}_0} \sum_{i \in \mathcal{K}} \sum_{m \in \mathcal{M}} y_{b,i} \bar{R}_{b,i,m}(\mathbf{x}^{(t)}) \\
\text{s.t. } &\bar{C}_1 : \sum_{b \in \mathcal{B}_0} \sum_{m \in \mathcal{M}} y_{b,i} \bar{R}_{b,i,m}(\mathbf{x}^{(t)}) \geq R_i^{\text{th}}, \\
&\bar{C}_2 : \sum_{m \in \mathcal{M}} \sum_{b' \in \mathcal{B}_0} y_{b',b} \bar{R}_{b',b,m}(\mathbf{x}^{(t)}) \\
&\quad - \sum_{m \in \mathcal{M}} \sum_{i \in \mathcal{I}} y_{b,i} \bar{R}_{b,i,m}(\mathbf{x}^{(t)}) \geq 0, \\
&C_3, C_4, C_{11}.
\end{aligned} \tag{26}$$

Note that (26) provides a tight lower bound as *Proposition 1*. Furthermore, it converges to KKT point of the original problem using an iterative algorithm since it provides a sequence of non-decreasing objective function value [38], [39]. Therefore, we focus on the lower bound of original problem.

However, (26) is still non-convex problem since it is the integer programming and \bar{C}_2 is non-convex due to the difference of two concave functions. To tackle the non-convexity of binary constraint first, we rewrite the constraint C_{11} into its equivalent form given as

$$\begin{aligned}
C_{11a} : &0 \leq x_{b,i,m} \leq 1, \quad \forall b \in \mathcal{B}_0, i \in \mathcal{I}, m \in \mathcal{M}, \\
C_{11b} : &\sum_{b \in \mathcal{B}_0} \sum_{i \in \mathcal{I}} \sum_{m \in \mathcal{M}} (x_{b,i,m} - x_{b,i,m}^2) \leq 0.
\end{aligned} \tag{27}$$

It should be noted that C_{11b} is non-convex constraint. Hence, we adopt the Lagrangian approach by adding a penalty term to the objective function [40], [41]. Accordingly, (26) can be rewritten as

$$\begin{aligned}
\max_{\mathbf{x}} \quad &\sum_{b \in \mathcal{B}_0} \sum_{m \in \mathcal{M}} \left(\sum_{i \in \mathcal{K}} y_{b,i} \bar{R}_{b,i,m}(\mathbf{x}^{(t)}) - \mu \sum_{i \in \mathcal{I}} (x_{b,i,m} - x_{b,i,m}^2) \right) \\
\text{s.t. } &\bar{C}_1, \bar{C}_2, C_3, C_4, C_{11a},
\end{aligned} \tag{28}$$

where μ is the penalty factor which penalizes the objective function for non-integer value of $x_{b,i,m}$.

Proposition 2: For sufficiently large value of μ , the optimization problem (28) is equivalent to (26).

Proof: See Appendix A

Since the objective function and \bar{C}_2 are still non-convex functions, we can rewrite (28) as

$$\begin{aligned}
\text{(P3-2)} \quad &\max_{\mathbf{x}} F(\mathbf{x}) - G(\mathbf{x}) \\
\text{s.t. } &f_b(\mathbf{x}) - g_b(\mathbf{x}) \geq 0, \quad \forall b \in \mathcal{B}, \\
&\bar{C}_1, C_3, C_4, C_{11a},
\end{aligned} \tag{29}$$

where $F(\mathbf{y})$, $G(\mathbf{x})$, $f_b(\mathbf{x})$, and $g_b(\mathbf{x})$ are defined as

$$\begin{aligned}
F(\mathbf{x}) &= \sum_{b \in \mathcal{B}_0} \sum_{m \in \mathcal{M}} \left(\sum_{i \in \mathcal{K}} y_{b,i} \bar{R}_{b,i,m}(\mathbf{x}^{(t)}) - \mu \sum_{i \in \mathcal{I}} x_{b,i,m} \right), \\
G(\mathbf{x}) &= -\mu \sum_{b \in \mathcal{B}_0} \sum_{i \in \mathcal{I}} \sum_{m \in \mathcal{M}} x_{b,i,m}^2, \\
f_b(\mathbf{x}) &= \sum_{b' \in \mathcal{B}_0} \sum_{m \in \mathcal{M}} y_{b',b} \bar{R}_{b',b,m}(\mathbf{x}^{(t)}), \\
g_b(\mathbf{x}) &= \sum_{i \in \mathcal{I}} \sum_{m \in \mathcal{M}} y_{b,i} \bar{R}_{b,i,m}(\mathbf{x}^{(t)}).
\end{aligned} \tag{30}$$

It can be observed that (29) is a form of the difference of two concave functions (DC) [42]. Since $F(\mathbf{x})$, $G(\mathbf{x})$, $f_b(\mathbf{x})$, and $g_b(\mathbf{x})$ are concave functions, (29) belongs to the class of DC programming (DCP) which can be solved using DC algorithm (DCA) [42]. Thus, we can construct a surrogate function for $G(\mathbf{x})$ and $g_b(\mathbf{x})$ by using the first order Taylor approximation given as

$$\begin{aligned}
G(\mathbf{x}) &\leq \bar{G}(\mathbf{x}, \mathbf{x}^{(t)}) = G(\mathbf{x}^{(t)}) + \nabla_{\mathbf{x}} G^T(\mathbf{x}^{(t)}) (\mathbf{x} - \mathbf{x}^{(t)}), \\
g_b(\mathbf{x}) &\leq \bar{g}_b(\mathbf{x}, \mathbf{x}^{(t)}) = g_b(\mathbf{x}^{(t)}) + \nabla_{\mathbf{x}} g_b^T(\mathbf{x}^{(t)}) (\mathbf{x} - \mathbf{x}^{(t)}).
\end{aligned} \tag{31}$$

As a result, the optimal SA can be obtained by solving the following convex problem.

$$\begin{aligned}
\text{(P3-3)} \quad &\max_{\mathbf{x}} F(\mathbf{x}) - \bar{G}(\mathbf{x}, \mathbf{x}^{(t)}) \\
\text{s.t. } &f_b(\mathbf{x}) - \bar{g}_b(\mathbf{x}, \mathbf{x}^{(t)}) \geq 0, \quad \bar{C}_1, C_3, C_4, C_{11a}.
\end{aligned} \tag{32}$$

This problem can be solved using the conventional optimization method such as interior point method [43], [44].

Proposition 3: The optimal solution of (32) is the subset of the feasible set of (29)

Proof: In the $(t+1)$ th iteration, the solution obtained from (32) is $\mathbf{x}^{(t+1)}$. It is noteworthy that $f_b(\mathbf{x}) - g_b(\mathbf{x}) \geq f_b(\mathbf{x}) - \bar{g}_b(\mathbf{x}, \mathbf{x}^{(t)})$ as in (31). Therefore, the constraint $f_b(\mathbf{x}^{(t+1)}) - \bar{g}_b(\mathbf{x}^{(t+1)}, \mathbf{x}^{(t)}) \geq 0$ in (32) guarantees $f_b(\mathbf{x}^{(t+1)}) - g_b(\mathbf{x}^{(t+1)}) \geq 0$ of (29).

$$\begin{aligned}
e_{b,i,m}(\mathbf{P}) &= y_{b,i} x_{b,i,m} \log_2 \left(\alpha_{b,i,m} P_{b,m} + \sum_{b' \in \mathcal{B}_0 \setminus \{b,i\}} \sum_{i' \in \mathcal{I} \setminus \{b,b',i\}} x_{b',i',m} \alpha_{b,b',i,i',m} P_{b',m} + \sigma^2 \right), \\
q_{b,i,m}(\mathbf{P}) &= y_{b,i} x_{b,i,m} \log_2 \left(\sum_{b' \in \mathcal{B}_0 \setminus \{b,i\}} \sum_{i' \in \mathcal{K} \setminus \{b,b',i\}} x_{b',i',m} \alpha_{b,b',i,i',m} P_{b',m} + \sigma^2 \right).
\end{aligned} \tag{35}$$

Algorithm 2 DCA-based iterative algorithm for SA

- 1: Initialize T_{\max} , penalty factor μ , and feasible point $\mathbf{x}^{(0)}$, \mathbf{y} , and \mathbf{P}
 - 2: Set $t = 0$
 - 3: **repeat**
 - 4: Calculate $\bar{R}_{b,i,m}(\mathbf{x}^{(t)})$, $\bar{G}(\mathbf{x}, \mathbf{x}^{(t)})$, and $\bar{g}_b(\mathbf{x}, \mathbf{x}^{(t)})$
 - 5: Solve the problem (32) and obtain the subchannel allocation policy $\{\mathbf{x}^{(t)*}\}$
 - 6: Set $t = t + 1$
 - 7: **until** convergence or $t = T_{\max}$
-

Proposition 4: The approximation of (31) gives a tight lower bound which provides the improved solution after each iteration and it converges to a local optimal point.

Proof: Recall that the objective function of (29) can be approximated as $F(\mathbf{x}) - G(\mathbf{x}) \geq F(\mathbf{x}) - \bar{G}(\mathbf{x}, \mathbf{x}^{(t)})$. For $\mathbf{x} = \mathbf{x}^{(t)}$, the equality holds, which means the tightness of the lower bound. Moreover, the solution of (32) gives the improved objective value at each iteration. For given $\mathbf{x}^{(t)}$, the optimal solution of (29) at the $(t+1)$ th iteration is $\mathbf{x}^{(t+1)}$. Then, we have

$$\begin{aligned}
&F(\mathbf{x}^{(t+1)}) - G(\mathbf{x}^{(t+1)}) \\
&\geq F(\mathbf{x}^{(t+1)}) - G(\mathbf{x}^{(t)}) - \nabla_{\mathbf{x}} G^T(\mathbf{x}^{(t+1)})(\mathbf{x}^{(t+1)} - \mathbf{x}^{(t)}) \\
&= \max_{\mathbf{x}} F(\mathbf{x}) - G(\mathbf{x}^{(t)}) - \nabla_{\mathbf{x}} G^T(\mathbf{x})(\mathbf{x} - \mathbf{x}^{(t)}) \\
&\geq F(\mathbf{x}^{(t)}) - G(\mathbf{x}^{(t)}) - \nabla_{\mathbf{x}} G^T(\mathbf{x}^{(t)})(\mathbf{x}^{(t)} - \mathbf{x}^{(t)}) \\
&\geq F(\mathbf{x}^{(t)}) - G(\mathbf{x}^{(t)}).
\end{aligned} \tag{33}$$

Thus, the solution of (32) provides the non-decreasing objective value as the iteration continues and it converges to a local optimal solution. Moreover, by adopting SCA based algorithm, all the constraints of (23) can be satisfied as in *Proposition 3*

It is worth noting that the lower bound will become tighter as the iteration continues. To tighten the obtained lower bound, we adopt the iterative algorithm which continues until convergence to a local optimum point. The detailed procedure is summarized in Algorithm 2.

C. Power Allocation

For given AO variable \mathbf{y} and SA variable \mathbf{x} , the PA problem can be reformulated as

$$\begin{aligned}
(\mathbf{P4}) \quad &\max_{\mathbf{P}} \sum_{b \in \mathcal{B}_0} \sum_{i \in \mathcal{K}} \sum_{m \in \mathcal{M}} y_{b,i} x_{b,i,m} R_{b,i,m} \\
&\text{s.t. } C_1, C_2, C_8, C_9.
\end{aligned} \tag{34}$$

Our aim for this subproblem is to obtain the optimal PA

that maximizes the sum rate under the constraints in (34). It is well-known that the water-filling algorithm is optimal PA method. However, we are not able to apply the conventional water-filling algorithm to our system model since there exist two kinds of interference (e.g., the cross-tier interference and the inter-cell interference) in IAB network. Therefore, we propose the iterative algorithm in consideration of cross-tier interference and inter-cell interference.

Note that (34) is a non-convex problem due to the non-convexity of the objective function and feasible set. To make the problem tractable, we reformulate the problem (34) into the form of DCP which can be solved by DCA. We first rewrite the objective function as

$$y_{b,i} x_{b,i,m} R_{b,i,m} = e_{b,i,m}(\mathbf{P}) - q_{b,i,m}(\mathbf{P}), \tag{36}$$

where $e_{b,i,m}(\mathbf{P})$ and $q_{b,i,m}(\mathbf{P})$ is defined as (35) at the top of the current page.

Using (36), (34) can be written in the form of DC as follows.

$$\begin{aligned}
(\mathbf{P4-1}) \quad &\max_{\mathbf{P}} E(\mathbf{P}) - Q(\mathbf{P}) \\
&\text{s.t. } E_i(\mathbf{P}) - Q_i(\mathbf{P}) \geq R_i^{\text{th}}, \forall i \in \mathcal{K}, \\
&\quad h_{1,b}(\mathbf{P}) - h_{2,b}(\mathbf{P}) \geq 0, \forall b \in \mathcal{B}, \\
&\quad C_8, C_9,
\end{aligned} \tag{37}$$

where

$$\begin{aligned}
E(\mathbf{P}) &= \sum_{b \in \mathcal{B}_0} \sum_{i \in \mathcal{K}} \sum_{m \in \mathcal{M}} e_{b,i,m}(\mathbf{P}), \\
Q(\mathbf{P}) &= \sum_{b \in \mathcal{B}_0} \sum_{i \in \mathcal{K}} \sum_{m \in \mathcal{M}} q_{b,i,m}(\mathbf{P}), \\
E_i(\mathbf{P}) &= \sum_{b \in \mathcal{B}_0} \sum_{m \in \mathcal{M}} e_{b,i,m}(\mathbf{P}), \\
Q_i(\mathbf{P}) &= \sum_{b \in \mathcal{B}_0} \sum_{m \in \mathcal{M}} q_{b,i,m}(\mathbf{P}), \\
h_{1,b}(\mathbf{P}) &= \sum_{b' \in \mathcal{B}_0} \sum_{m \in \mathcal{M}} e_{b',b,m}(\mathbf{P}) + \sum_{i \in \mathcal{I}} \sum_{m \in \mathcal{M}} q_{b,i,m}(\mathbf{P}), \\
h_{2,b}(\mathbf{P}) &= \sum_{b' \in \mathcal{B}_0} \sum_{m \in \mathcal{M}} q_{b',b,m}(\mathbf{P}) + \sum_{i \in \mathcal{I}} \sum_{m \in \mathcal{M}} e_{b,i,m}(\mathbf{P}).
\end{aligned} \tag{38}$$

Since $e_{b,i,m}(\mathbf{P})$ and $q_{b,i,m}(\mathbf{P})$ are concave functions, all the functions in (38) are concave and (37) can be considered as DCP. We approximate $Q(\mathbf{P})$, $Q_i(\mathbf{P})$, and $h_{2,b}(\mathbf{P})$ using the first order Taylor series around the point $\mathbf{P}^{(t)}$ given as

$$\begin{aligned}
Q(\mathbf{P}) &\leq \bar{Q}(\mathbf{P}, \mathbf{P}^{(t)}) = Q(\mathbf{P}^{(t)}) + \nabla_{\mathbf{P}} Q^T(\mathbf{P}^{(t)})(\mathbf{P} - \mathbf{P}^{(t)}), \\
Q_i(\mathbf{P}) &\leq \bar{Q}_i(\mathbf{P}, \mathbf{P}^{(t)}) = Q_i(\mathbf{P}^{(t)}) + \nabla_{\mathbf{P}} Q_i^T(\mathbf{P}^{(t)})(\mathbf{P} - \mathbf{P}^{(t)}), \\
h_{2,b}(\mathbf{P}) &\leq \bar{h}_{2,b}(\mathbf{P}, \mathbf{P}^{(t)}) = h_{2,b}(\mathbf{P}^{(t)}) + \nabla_{\mathbf{P}} h_{2,b}^T(\mathbf{P}^{(t)})(\mathbf{P} - \mathbf{P}^{(t)}).
\end{aligned} \tag{39}$$

$$O\left(I_1(BK + K) + I\left(I_2(B^2M + (K + 1)BM + KM) + I_3(BM + M)\right) \log \epsilon^{-1}\right). \quad (41)$$

Algorithm 3 Joint AO, SA, and PA algorithm for MH-IAB network

- 1: Initialize $t = 0$, T_{\max} and feasible $\mathbf{y}^{(0)}$, $\mathbf{x}^{(0)}$, and $\mathbf{P}^{(0)}$.
 - 2: **repeat**
 - 3: Set $t = t + 1$
 - 4: Obtain the optimal $\mathbf{y}^{(t+1)}$ using (19) with given $\mathbf{P}^{(t)}$ and $\mathbf{x}^{(t)}$.
 - 5: Solve the problem (32) for given $\mathbf{y}^{(t+1)}$ and $\mathbf{P}^{(t)}$ to obtain $\mathbf{x}^{(t+1)}$
 - 6: Solve the problem (40) for given $\mathbf{y}^{(t+1)}$ and $\mathbf{x}^{(t+1)}$ and obtain the optimal $\mathbf{P}^{(t+1)}$
 - 7: **until** convergence or $t = T_{\max}$
-

Then, the approximated problem at the t th iteration can be written as

$$\begin{aligned}
 (\mathbf{P4-2}) \quad & \max_{\mathbf{P}} E(\mathbf{P}) - \bar{Q}(\mathbf{P}, \mathbf{P}^{(t)}) \\
 \text{s.t.} \quad & E_i(\mathbf{P}) - \bar{Q}_i(\mathbf{P}, \mathbf{P}^{(t)}) \geq R_i^{\text{th}}, \\
 & h_{1,b}(\mathbf{P}) - \bar{h}_{2,b}(\mathbf{P}, \mathbf{P}^{(t)}) \geq 0, \\
 & C_8, C_9.
 \end{aligned} \quad (40)$$

Note that (40) is a convex problem which can be solved by conventional convex approach such as interior-point method. According to *Proposition 3*, the feasible points of (40) are the subset of the feasible points of (34). It should be also noted that the solution of (40), which is obtained by the iterative algorithm similar to Algorithm 2, converges to a KKT point of the original problem given in (34) [45].

D. Overall Algorithm

In the previous subsections, we proposed the low complexity algorithms for AO, SA, and PA. The original problem in (12) is decomposed into the three subproblems of (13), (23), and (34) where the Lagrangian approach based algorithm is proposed for AO subproblem, and DCA based iteration algorithms are proposed for SA and PA subproblems. We also showed that the optimal solution for AO can be obtained and the local optimal solution of the SA and PA can be achieved. Now, we propose an alternating algorithm which jointly optimizes AO, SA, and PA by solving each subproblem in an iterative manner. The detail of the overall algorithm is summarized in Algorithm 3 and the convergence behavior of proposed algorithm is shown in Section V.

E. Complexity Analysis

The computational complexity of the block coordinate descent-based approach in Algorithm 3 lies mainly in Algorithm 1 and Algorithm 2. For Algorithm 1, considering that the total iterative number in Algorithm 1 is I_1 , the computational complexity of AO is given by $O(I_1(BK+K))$. For Algorithm 2,

TABLE II
SYSTEM PARAMETERS.

Notation	Parameter	Value
M	Number of subchannels	50
B	Number of SBSs	4, 8
K	Number of UEs	[10, 50]
N_m	Number of antennas for MBS	64
N_s	Number of antennas with SBS	16
N_u	Number of antennas with UE	2
L	Number of NLoS paths	6
P_0^{\max}	Maximum transmit power of MBS	46 dBm
P_b^{\max}	Maximum transmit power of SBS	30 dBm
W	Bandwidth per subchannel	2 MHz
N_0	Noise variance	-174 dBm/Hz
f_c	Carrier frequency	28 GHz
β_{LoS}	Path loss exponent of LoS path	2.1
β_{NLoS}	Path loss exponent of NLoS path	3.17
σ_{LoS}	Shadowing standard deviation of LoS path	3.76 dB
σ_{NLoS}	Shadowing standard deviation of NLoS path	8.09 dB

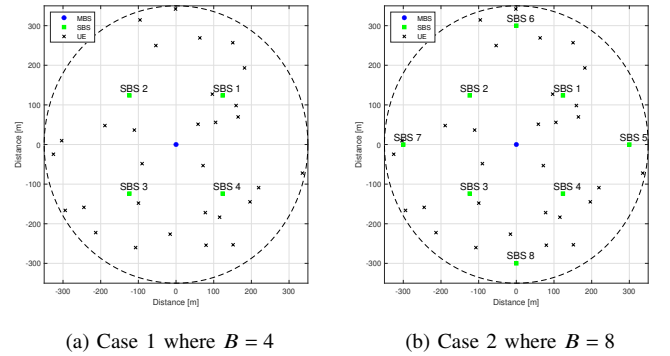


Fig. 3. The deployments of MBS and SBSs for different number of SBSs where dotted line represents the coverage area of MBS.

it involves solving the convex problem given in (32) where the dimension of optimization variable is $B^2M + (K + 1)BM + KM$. By using a primal-dual interior point method to address the convex problem, the computational complexity of SA is $O\left(I_2(B^2M + (K + 1)BM + KM) \log \epsilon^{-1}\right)$, in which I_2 and ϵ represent the number of iteration in Algorithm 2 and the determined accepted duality gap, respectively [44]. Likewise, the computational complexity of PA is given by $O\left(I_3(BM + M) \log \epsilon^{-1}\right)$, where I_3 is the number of iteration for (40). Thus, given the total iteration number is I , the computational complexity of Algorithm 3 is derived as (41).

V. SIMULATION RESULTS

In our simulations, MBS is located at the center with radius 350 m and SBSs are located in a fixed position as in Fig. 3

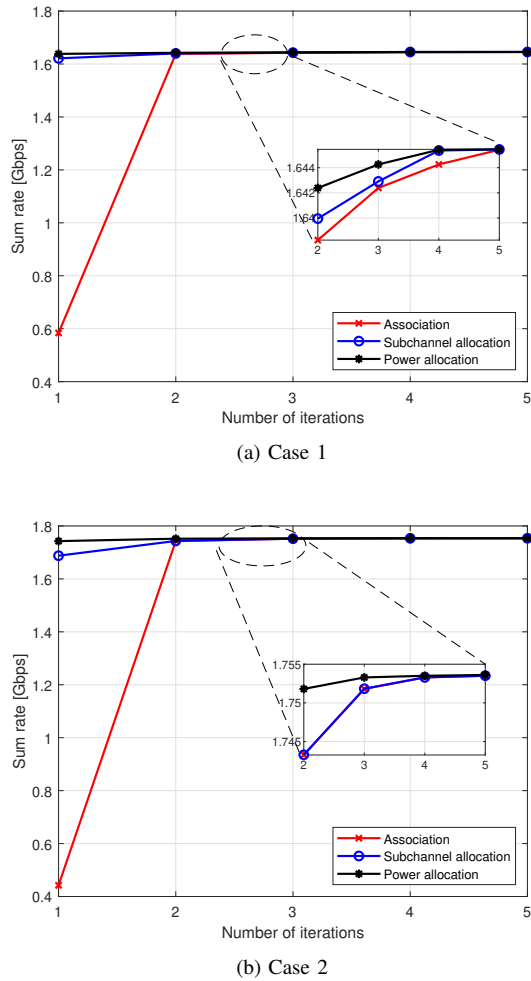


Fig. 4. Convergence behavior for the proposed Algorithm 3 where $R_i^{\text{th}} = 2$ Mbps and $K = 30$.

where 4 SBSs and 8 SBSs are deployed for Case 1 and Case 2, respectively. Unless otherwise specified, we adopt the simulation parameters given in Table II. Moreover, maximum ratio transmission (MRT) precoding and maximal ratio combining (MRC) are employed for transmitter and receiver, respectively.³

A. Snapshot of MH-IAB Network

In the case of fixed UE location as in Fig. 3, we show the convergence of our proposed Algorithm 3 in Fig. 4 where the optimization results for AO, SA, and PA, i.e., $\{\mathbf{y}, \mathbf{x}, \mathbf{P}\}$, are getting close in each iteration, as the number of iteration increases, and are converged in the 5 iterations as seen in Fig. 4. Therefore, we can confirm that the optimization results for \mathbf{y} , \mathbf{x} , and \mathbf{P} in each step are monotonically increasing, and the joint optimization algorithm converges.

³In order to mitigate the interference in the IAB network, zero-forcing (ZF) and minimum mean square error (MMSE) beamforming techniques can be employed but it does not affect to the proposed algorithms. Therefore, we assume MRT and MRC in this work and we focus on the IAB network design concerning association and resource allocation to validate our proposed algorithms.

Fig. 5 shows the results of proposed association algorithm under different minimum rate requirements and MBS transmit power for Case 1 and Case 2. In particular, we set the number of UEs as $K = 30$ because it provides the best performance as illustrated in Fig. 7 and is also an appropriate number considering the simulation complexity. In the low data rate required case as shown in Figs. 5(a) and 5(d), UEs tend to associate with MBS since it provides a better link quality due to high transmit power and the wired backhaul of MBS. On the other hand, in the case that high data rate is required shown in Figs. 5(b) and 5(e), UEs are likely to access the nearest BSs as long as there is no LoS path for UE. Although MBS provides better link quality than SBS, MBS cannot simultaneously support a large number of UEs to meet high data rate requirements using the limited resources. Thus, it is better to associate UE with lightly loaded SBSs for high data rate requirements to exploit the spatial reuse of limited resources as in Figs. 5(b) and 5(e). Moreover, we demonstrate that most of UEs are associated with the nearest BSs when MBS has the same transmit power with SBS as in Figs. 5(d) and 5(f), while UEs require low data rate. In other words, there is no gain to associate with MBS unless the LoS path is guaranteed. Note that in Fig. 5, there are blockages of backhaul link that determine whether the LoS path for backhaul link is guaranteed or not. From the results in Fig. 5, we observe that the backhaul links are configured by circumventing the NLoS link to enhance the backhaul throughput. For example, “SBS 3” connects to “SBS 8” in Case 2 since the LoS path from “SBS 3” to MBS is blocked by an obstacle.

B. Performance Evaluation of IAB Network

Throughout this subsection, our proposed scheme is compared with alternative schemes as follows.

- 1) **SH/MH with max SINR** is the case where the backhaul links are configured by “Single-hop (SH)” (i.e., SBSs are directly connected to MBS) or “Multi-hop (MH)” and the access links are configured by “max SINR” based association scheme where each UE selects the BS providing the largest SINR link.
- 2) **SH/MH with matching** is the case where the matching-based algorithm is used for configuring the backhaul and access links. In particular, the algorithm in [25] is used for MH backhauling while the algorithm in [46] is utilized for access link.
- 3) **SH/MH with prop** implies the case where the proposed association scheme configures the backhaul and access links as in Algorithm 1.

It is noted that the proposed SA and PA algorithms are adopted for all the baselines. Also, the numerical results are obtained by averaging over the random location of UEs where they are uniformly distributed in a cell.

Table. III represents the LoS probability of backhaul and access links achieved by the baselines and the proposed scheme. As seen in Table. III, the LoS probability of backhaul is significantly increased by configuring the MH backhaul links, and particularly it can be further increased when a large number of SBSs are deployed. Since each SBS is more likely to obtain the

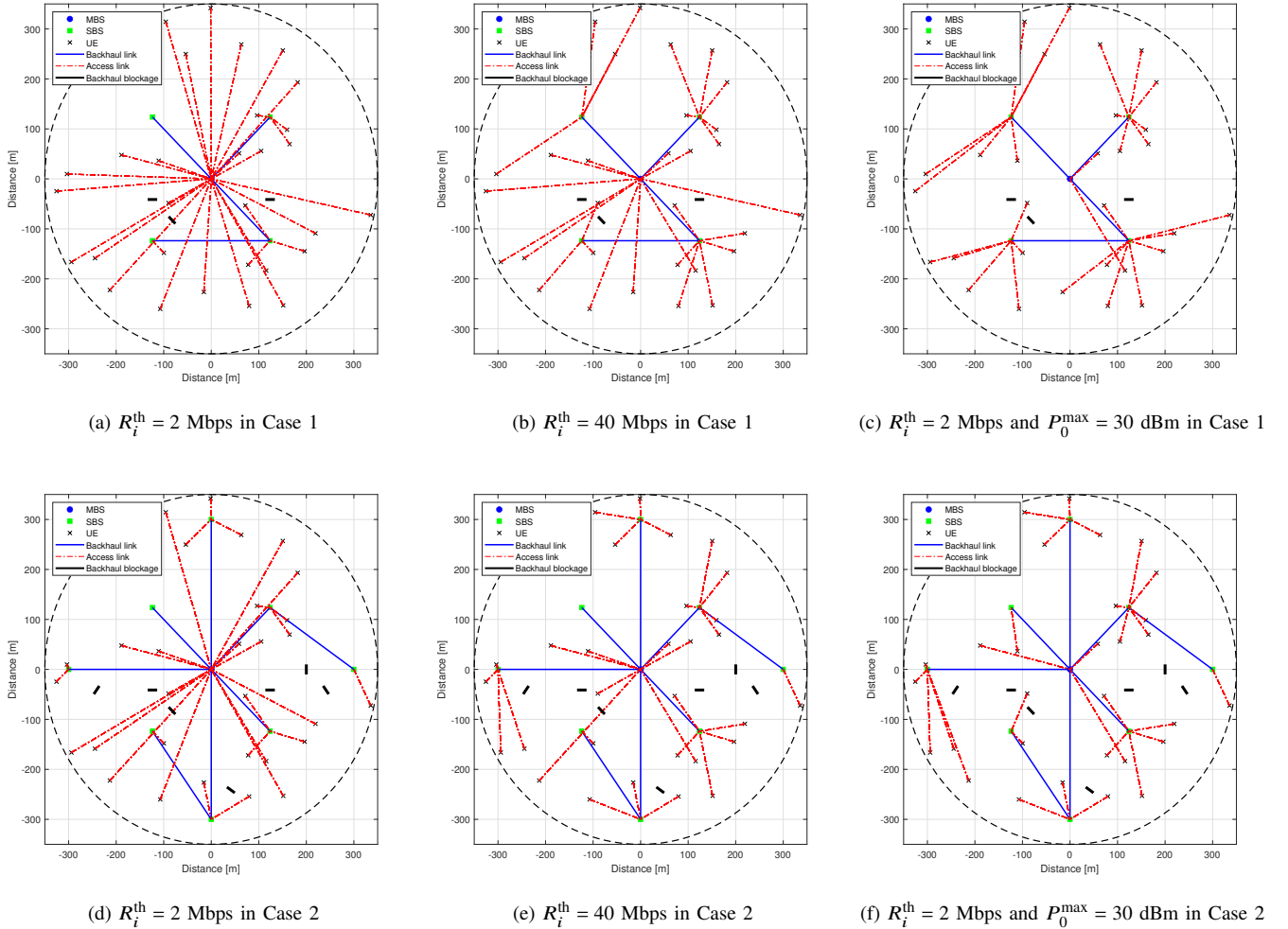


Fig. 5. Examples of AO results obtained by Algorithm 1 for various minimum rate requirements and MBS transmit power where $K = 30$.

LoS backhaul link under the dense SBS deployment scenario, the proposed association scheme achieves high LoS probability of backhaul by connecting the LoS path between SBSs. For the access link, we compare the proposed scheme with “max SINR” and “direct access” that connects all the UEs to MBS. As in Table. III, the LoS probability of access link can be enhanced using the IAB network compared to direct access. However, the LoS probability of proposed scheme slightly decreases compared with the max SINR scheme. Although some UEs are associated with BS which provides the NLoS link, the proposed scheme achieves better system throughput because access links are configured by taking into account the backhaul capacity and the load of SBSs as in Fig. 7. Therefore, the coverage can be extended using IAB network with the proposed association scheme by providing high LoS probability for both backhaul and access links.

Fig. 6 demonstrates the performance of various algorithms by comparing them with an exhaustive search. For an exhaustive search, we set the simulation parameters as $M = 10$ and $K = 2, 3, 4$ in Case 1 due to its high complexity. It is shown that the proposed algorithm provides a higher sum rate while its performance is closer to an exhaustive search than

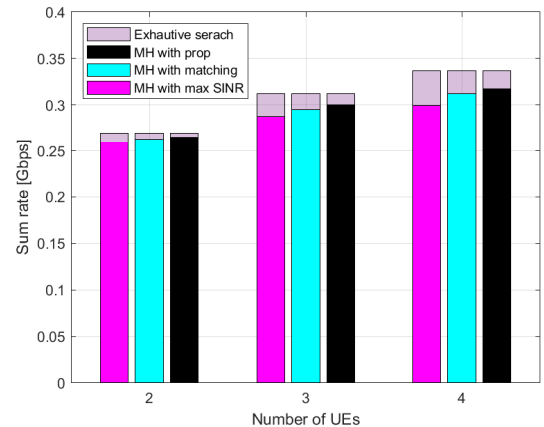
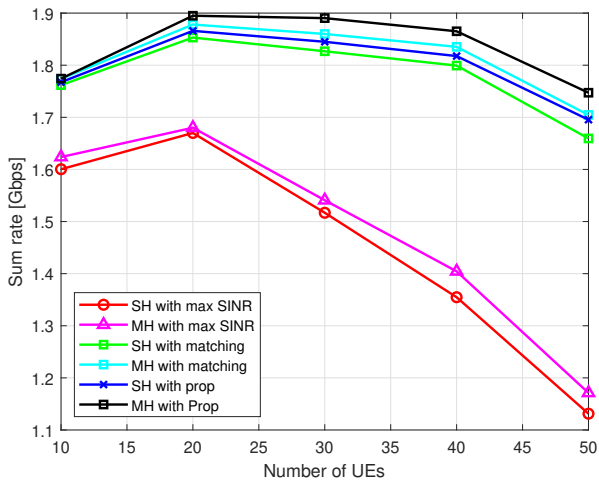


Fig. 6. Comparison of different algorithms with an exhaustive search for Case 1.

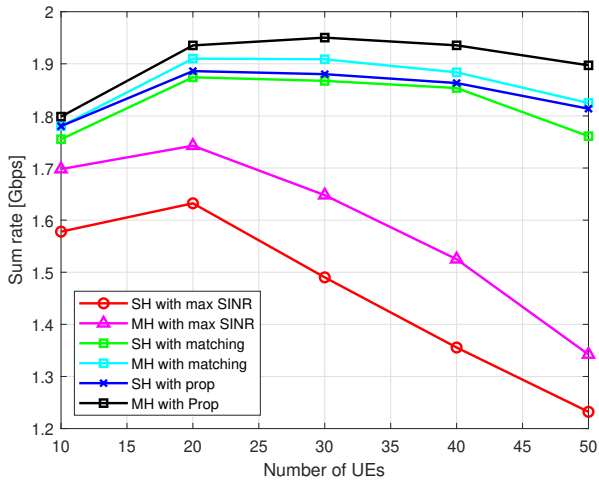
the other baselines. It is worth noting that the gap between an exhaustive search and our proposed algorithm becomes wider as the number of UEs increases while the result of our proposed scheme is close to the global optimum even with

TABLE III
COMPARISON OF LOS PROBABILITY FOR BACKHAUL AND ACCESS LINKS.

Association Scheme		LoS probability for Case 1	LoS probability for Case 2
Backhaul Link	Single-Hop	0.6335	0.4778
	Multi-Hop	0.8175	0.8400
Association Scheme		LoS probability for Case 1	LoS probability for Case 2
Access Link	Direct Access	0.1446	0.1446
	Max SINR	0.3246	0.4740
	Proposed	0.3242	0.4575



(a) Case 1 where $B = 4$



(b) Case 2 where $B = 8$

Fig. 7. Comparison of sum rate for different number of UEs where $R_i^{\text{th}} = 2$ Mbps.

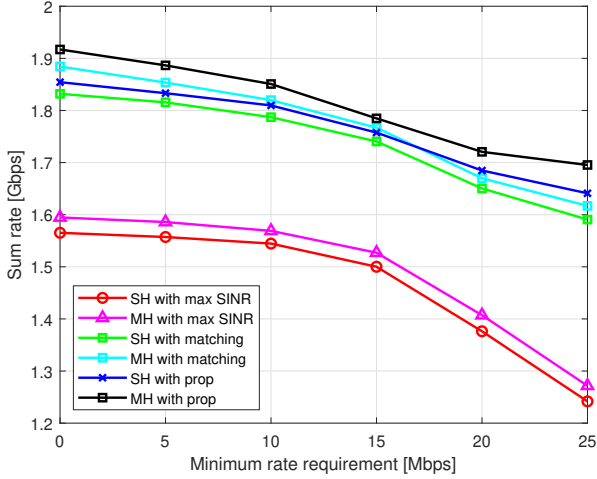
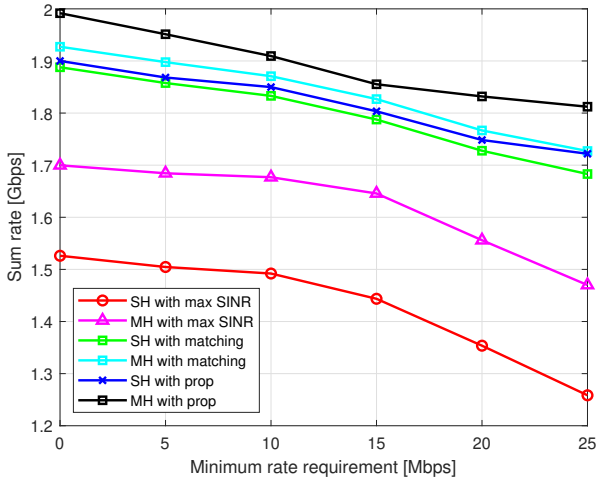
low computational complexity.

In Fig. 7, we compare the MH backhauling based proposed scheme with the benchmarks with respect to the number of UEs. We observe two trends as the number of UEs increases: *i*)

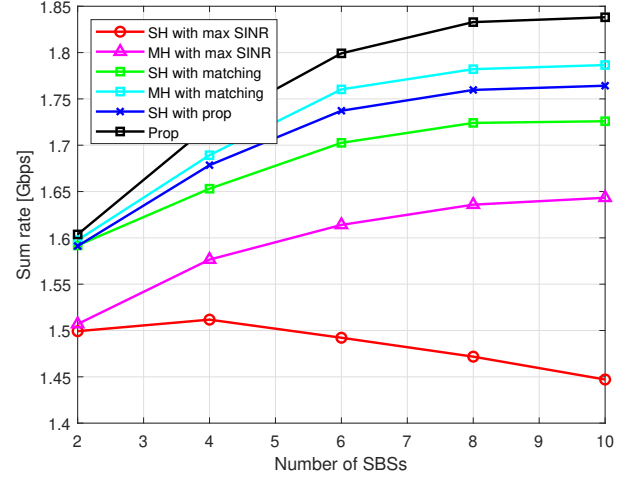
the sum rate increases due to the multi-user diversity in all the schemes, and *ii*) it decreases when a large number of UEs are deployed since the limited resource is not enough to support all the UEs' minimum rate requirements. In particular, this phenomenon becomes more severe for max SINR association scheme because it does not consider the limitation of backhaul capacity and the load of SBSs even if the MH backhauling is supported. In contrast, the performance of sum rate using the proposed scheme is significantly boosted compared to max SINR association scheme even if the SH backhauling is used. Interestingly, both the matching-based method and proposed scheme show a similar trend but our proposed algorithm achieves a better performance. It highlights that the proposed scheme adaptively configures the access links to resolve the bottleneck of backhaul link while efficiently allocating the resources to satisfy the UEs' requirements.

In Fig. 8, we evaluate the sum rate over the minimum rate requirements. It is shown that the sum rate decreases as the minimum rate requirement increases and the MH backhauling based proposed scheme outperforms the other baselines. Thus, the MH backhauling by deploying a large number of SBSs provides a better performance under QoS constraints. From Figs. 7 and 8, we confirm that the proposed scheme achieves better sum rate performance in a dense UE deployment case even though max SINR association scheme achieves higher LoS probability. The proposed scheme distributedly associates UEs with lightly loaded SBS regardless of backhauling scheme to exploit the spatial reuse of limited spectrum resources. We here point out that the consideration of backhaul condition in UE association is important to enhance the system performance in the IAB network. Additionally, we demonstrate that the sum rate performance can be improved by deploying many SBSs and configuring the MH backhauling regardless of UE association scheme. However, the dense SBS deployment scenario with "SH with max SINR" reduces the sum rate performance with the small number of UEs since it provides a low LoS probability of backhaul as in Table. III.

Fig. 9 illustrates the sum rate performance with respect to the number of SBSs for different association schemes. As shown in Fig. 9, the sum rate increases as the number of SBSs increases by employing the MH backhauling or the proposed association scheme for access links. On the other hand, "SH with max SINR" rather deteriorates the system throughput in

(a) Case 1 where $B = 4$ (b) Case 2 where $B = 8$ Fig. 8. Sum rate versus minimum rate requirement where $K = 30$.

which more SBSs are deployed, such as ultra-dense network, since it cannot exploit the backhaul conditions. It is noted that the performance of proposed scheme increases as the number of SBSs increases. We here point out that proposed algorithm exploits the spatial diversity gain by configuring MH backhauling or access links to enhance the link quality. Besides, we also highlight that the proposed UE association scheme significantly improves the system throughput since it associates UEs by considering the backhaul traffic and offloading the traffic from MBS to SBSs. Note that matching-based algorithm also enhance the system throughput even if SH backhauling is employed while our proposed algorithm still provides the best performance. As a final remark, we validate that the proposed algorithm efficiently supports the MH backhaul connectivity in IAB network, which improves the system throughput by circumventing the blockage and offloading UEs to SBSs.

Fig. 9. Comparison of sum rate performance for different number of SBSs where $R_i^h = 2$ Mbps and $K = 30$.

VI. CONCLUSION

In this paper, we have investigated the joint association and resource allocation for IAB network in consideration of MH backhauling. To maximize the sum rate of IAB network, the joint optimization problem is decomposed into three subproblems. First, we used Lagrangian duality approach to address AO for backhaul and access links to configure the MH wireless backhaul links. Then, by using SCA approach, we tackled the resource allocation including SA and PA. Simulation results showed that the proposed algorithm provides more spectral-efficient association results and it also achieves the diversity gain. Furthermore, the proposed algorithm for the IAB network outperforms the conventional schemes by enabling the efficient MH backhauling and offloading UEs from MBS to SBSs.

APPENDIX A

We prove *Proposition 1* using the abstract Lagrangian duality. The primal solution of (28) is given as

$$p^* = \max_{\mathbf{x}} \min_{\mu} L(\mathbf{x}, \mu). \quad (42)$$

Also, the solution of dual problem can be written as

$$d^* = \min_{\mu} \max_{\mathbf{x}} L(\mathbf{x}, \mu) = \min_{\mu} \theta(\mu), \quad (43)$$

where $\theta(\mu) = \max_{\mathbf{x}} L(\mathbf{x}, \mu)$. According to the weak duality, $d^* \geq p^*$ always holds. Note that we have $\sum_{b \in \mathcal{B}_0} \sum_{i \in \mathcal{I}} \sum_{m \in \mathcal{M}} (x_{b,i,m} - x_{b,i,m}^2) \geq 0$ for \mathbf{x} such that $\bar{C}_1, \bar{C}_2, C_3, C_4$, and C_{11a} . Thus, two cases can be considered

Case 1: Let us consider $\sum_{b \in \mathcal{B}_0} \sum_{i \in \mathcal{I}} \sum_{m \in \mathcal{M}} (x_{b,i,m} - x_{b,i,m}^2) = 0$. In this case, $L(\mathbf{x}, \mu) = \min_{\mu} L(\mathbf{x}, \mu)$ holds. Also, the following inequality holds

$$d^* = \min_{\mu} \max_{\mathbf{x}} L(\mathbf{x}, \mu) \leq \max_{\mathbf{x}} L(\mathbf{x}, \mu). \quad (44)$$

Substituting $L(\mathbf{x}, \mu) = \min_{\mu} L(\mathbf{x}, \mu)$ into the right side of (44) yields

$$\min_{\mu} \max_{\mathbf{x}} L(\mathbf{x}, \mu) \leq \max_{\mathbf{x}} \min_{\mu} L(\mathbf{x}, \mu). \quad (45)$$

By comparing the weak duality condition with (45), the strong duality holds as follows.

$$d^* = \min_{\mu} \max_{\mathbf{x}} L(\mathbf{x}, \mu) = \max_{\mathbf{x}} \min_{\mu} L(\mathbf{x}, \mu) = p^*. \quad (46)$$

Note that $\theta(\mu)$ is monotonically decreasing function with respect to μ . Since $d^* = \min_{\mu} \theta(\mu)$ as in (43), we conclude that $\theta(\mu) = d^*$ for $\mu \geq \mu^*$ where $\mu^* = \arg \min_{\mu} \theta(\mu)$.

Case 2: For the case of $\sum_{b \in \mathcal{B}_0} \sum_{i \in \mathcal{I}} \sum_{m \in \mathcal{M}} (x_{b,i,m} - x_{b,i,m}^2) > 0$. $\theta(\mu^*)$ tends to $-\infty$ due to monotonically decreasing function of $\theta(\mu)$. However, it contradicts the weak duality since the lower bound of $\theta(\mu)$ is p^* which is always greater than zero. Therefore, $\sum_{b \in \mathcal{B}_0} \sum_{i \in \mathcal{I}} \sum_{m \in \mathcal{M}} (x_{b,i,m} - x_{b,i,m}^2) = 0$ holds at the optimal point.

REFERENCES

- [1] J. G. Andrews *et al.*, "What will 5G be?" *IEEE J. Sel. Areas Commun.*, vol. 32, no. 6, pp. 1065–1082, Jun. 2014.
- [2] X. Wang *et al.*, "Millimeter wave communication: A comprehensive survey," *IEEE Commun. Surv. Tut.*, vol. 20, no. 3, pp. 1616–1653, Jun. 2018.
- [3] M. Baianifar, S. M. Razavizadeh, H. Akhlaghpasand, and I. Lee, "Energy efficiency maximization in mmWave wireless networks with 3D beamforming," *J. Commun. Netw.*, vol. 21, no. 2, pp. 125–135, Apr. 2019.
- [4] C. Dehos, J. L. González, A. D. Domenico, D. Kténas, and L. Dussot, "Millimeter-wave access and backhauling: The solution to the exponential data traffic increase in 5G mobile communications systems?" *IEEE Commun. Mag.*, vol. 52, no. 9, pp. 88–95, Sep. 2014.
- [5] Y. Niu, C. Gao, Y. Li, L. Su, and D. Jin, "Exploiting multi-hop relaying to overcome blockage in directional mmWave small cells," *J. Commun. Netw.*, vol. 18, no. 3, pp. 364–374, Jun. 2016.
- [6] A. Dammjanovic *et al.*, "A survey on 3GPP heterogeneous networks," *IEEE Wireless Commun.*, vol. 18, no. 3, pp. 10–21, Jun. 2011.
- [7] Z. Gao *et al.*, "MmWave massive-MIMO-based wireless backhaul for the 5G ultra-dense network," *IEEE Wireless Commun.*, vol. 22, no. 5, pp. 13–21, Oct. 2015.
- [8] Y. Wang *et al.*, "Triple-band scheduling with millimeter wave and terahertz bands for wireless backhaul," *J. Commun. Netw.*, vol. 24, no. 4, pp. 438–450, Aug. 2022.
- [9] B. Li, D. Zhu, and P. Liang, "Small cell in-band wireless backhaul in massive MIMO systems: A cooperation of next-generation techniques," *IEEE Trans. Wireless Commun.*, vol. 14, no. 12, pp. 7057–7069, Dec. 2015.
- [10] *NR—Study on Integrated Access and Backhaul*, document TR 38.874, 3GPP, 2017.
- [11] C. Saha and H. S. Dhillon, "Millimeter wave integrated access and backhaul in 5G: Performance analysis and design insights," *IEEE J. Sel. Areas Commun.*, vol. 37, no. 12, pp. 2669–2684, Dec. 2019.
- [12] M. Cudak, A. Ghosh, A. Ghosh, and J. Andrews, "Integrated access and backhaul: A key enabler for 5G millimeter-wave deployments," *IEEE Commun. Mag.*, vol. 59, no. 4, pp. 88–94, Apr. 2021.
- [13] K. Lee, S. Baek, and S. Bahk, "Mobility management of multi-hop mobile integrated access and backhaul network," *J. Commun. Netw.*, vol. 24, no. 4, pp. 475–488, Aug. 2022.
- [14] M. Polese *et al.*, "Integrated access and backhaul in 5G mmWave networks: Potential and challenges," *IEEE Commun. Mag.*, vol. 58, no. 3, pp. 62–68, Mar. 2020.
- [15] M. Pagin, T. Zugno, M. Polese, and M. Zorzi, "Resource management for 5G NR integrated access and backhaul: A semi-centralized approach," *IEEE Trans. Wireless Commun.*, vol. 21, no. 2, pp. 753–767, Feb. 2021.
- [16] J. Y. Lai, W.-H. Wu, and Y. T. Su, "Resource allocation and node placement in multi-hop heterogeneous integrated-access-and-backhaul networks," *IEEE Access*, vol. 8, pp. 122937–122958, Jul. 2020.
- [17] M. Polese, M. Giordani, A. Roy, D. Castor, and M. Zorzi, "Distributed path selection strategies for integrated access and backhaul at mmWaves," in *Proc. IEEE GLOBECOM*, Dec. 2018.
- [18] B. Lim and Y.-C. Ko, "Link association for small cell networks with wireless backhaul," in *Proc. ICTC*, Oct. 2021.
- [19] C. Saha, M. Afshang, and H. S. Dhillon, "Bandwidth partitioning and downlink analysis in millimeter wave integrated access and backhaul for 5G," *IEEE Trans. Wireless Commun.*, vol. 17, no. 12, pp. 8195–8210, Dec. 2018.
- [20] W. Pu, X. Li, J. Yuan, and X. Yang, "Resource allocation for millimeter wave self-backhaul network using markov approximation," *IEEE Access*, vol. 7, pp. 61283–61295, May 2019.
- [21] T. M. Nguyen, A. Yadav, W. Ajib, and C. Assi, "Resource allocation in two-tier wireless backhaul heterogeneous networks," *IEEE Trans. Wireless Commun.*, vol. 15, no. 10, pp. 6690–6704, Oct. 2016.
- [22] U. Siddique, H. Tabassum, and E. Hossain, "Downlink spectrum allocation for in-band and out-band wireless backhauling of full-duplex small cells," *IEEE Trans. Commun.*, vol. 65, no. 8, pp. 3538–3554, Aug. 2017.
- [23] N. Wang, E. Hossain, and V. K. Bhargava, "Joint downlink cell association and bandwidth allocation for wireless backhauling in two-tier HetNets with large-scale antenna arrays," *IEEE Trans. Wireless Commun.*, vol. 15, no. 5, pp. 3251–3268, May 2016.
- [24] W. Pu, X. Li, J. Yuan, and X. Yang, "Traffic-oriented resource allocation for mmWave multi-hop backhaul networks," *IEEE Commun. Lett.*, vol. 22, no. 11, pp. 2330–2333, Nov. 2018.
- [25] O. Semiari, W. Saad, M. Bennis, and Z. Dawy, "Inter-operator resource management for millimeter wave multi-hop backhaul networks," *IEEE Trans. Wireless Commun.*, vol. 16, no. 8, pp. 5258–5272, Aug. 2017.
- [26] *NG-RAN; Architecture description*, document TS 38.401, 3GPP, 2020.
- [27] C. Madapatha *et al.*, "On integrated access and backhaul networks: Current status and potentials," *IEEE Open J. Commun. Soc.*, vol. 1, pp. 1374–1389, Sep. 2020.
- [28] Z. Zhou, M. Dong, K. Ota, G. Wang, and L. T. Yang, "Energy-efficient resource allocation for D2D communications underlying cloud-RAN-based LTE-A networks," *IEEE Internet Things J.*, vol. 3, no. 3, pp. 428–438, Jun. 2016.
- [29] T. S. Rappaport *et al.*, "Overview of millimeter wave communications for fifth-generation (5G) wireless networks—with a focus on propagation models," *IEEE Trans. Antennas Propag.*, vol. 65, no. 12, pp. 6213–6230, Dec. 2017.
- [30] *Further advancements for E-UTRA physical layer aspects*, document TR 36.814, 3GPP, 2017.
- [31] U. Siddique, H. Tabassum, and E. Hossain, "Downlink spectrum allocation for in-band and out-band wireless backhauling of full-duplex small cells," *IEEE Trans. Commun.*, vol. 65, no. 8, pp. 3538–3554, Aug. 2017.
- [32] N. Saquib, E. Hossain, L. B. Le, and D. I. Kim, "Interference management in OFDMA femtocell networks: Issues and approaches," *IEEE Wireless Commun.*, vol. 19, no. 3, pp. 86–95, Jun. 2012.
- [33] Y. Pochet and L. A. Wolsey, *Production planning by mixed integer programming*. Springer Science & Business Media, 2006.
- [34] Wei Yu and R. Lui, "Dual methods for nonconvex spectrum optimization of multicarrier systems," *IEEE Trans. Commun.*, vol. 54, no. 7, pp. 1310–1322, Jul. 2006.
- [35] S. Boyd and A. Mutapcic, *Subgradient Methods*. Stanford, 2008.
- [36] B. R. Marks and G. P. Wright, "A general inner approximation algorithm for nonconvex mathematical programs," *Operations Research*, vol. 26, no. 4, pp. 681–683, Aug. 1978.
- [37] Z. Sheng, H. D. Tuan, A. A. Nasir, T. Q. Duong, and H. V. Poor, "Power allocation for energy efficiency and secrecy of wireless interference networks," *IEEE Trans. Wireless Commun.*, vol. 17, no. 6, pp. 3737–3751, Jun. 2018.
- [38] L. Xu, W. Yin, X. Zhang, and Y. Yang, "Fairness-aware throughput maximization over cognitive heterogeneous NOMA networks for industrial cognitive IoT," *IEEE Trans. Commun.*, vol. 68, no. 8, pp. 4723–4733, Aug. 2020.
- [39] K. Singh, A. Gupta, and T. Ratnarajah, "QoS-driven resource allocation and EE-balancing for multiuser two-way amplify-and-forward relay networks," *IEEE Trans. Wireless Commun.*, vol. 16, no. 5, pp. 3189–3204, May 2017.
- [40] B. Khamidehi, A. Rahmati, and M. Sabbaghian, "Joint sub-channel assignment and power allocation in heterogeneous networks: An efficient optimization method," *IEEE Commun. Lett.*, vol. 20, no. 12, pp. 2490–2493, Dec. 2016.

- [41] A. Khalili, S. Zarandi, and M. Rasti, "Joint resource allocation and offloading decision in mobile edge computing," *IEEE Commun. Lett.*, vol. 23, no. 4, pp. 684–687, Apr. 2019.
- [42] H. H. Kha, H. D. Tuan, and H. H. Nguyen, "Fast global optimal power allocation in wireless networks by local D.C. programming," *IEEE Trans. Wireless Commun.*, vol. 11, no. 2, pp. 510–515, Feb. 2012.
- [43] M. Grant and S. Boyd, "CVX: Matlab software for disciplined convex programming, version 2.1," <http://cvxr.com/cvx>, Mar. 2014.
- [44] S. Boyd, S. P. Boyd, and L. Vandenberghe, *Convex optimization*. Cambridge university press, 2004.
- [45] F. Wang, W. Chen, H. Tang, and Q. Wu, "Joint optimization of user association, subchannel allocation, and power allocation in multi-cell multi-association OFDMA heterogeneous networks," *IEEE Trans. Commun.*, vol. 65, no. 6, pp. 2672–2684, Jun. 2017.
- [46] M. K. Elhattab *et al.*, "A matching game for device association and resource allocation in heterogeneous cloud radio access networks," *IEEE Commun. Lett.*, vol. 22, no. 8, pp. 1664–1667, Aug. 2018.



Ki-Hun Kim received a B.S. degree, Information and Communication Engineering from Myongji University, Korea, in 2002, and M.S. degrees in IT Convergence Engineering from Aju University, Korea, in 2015. Currently he works at Hanwha Systems, Korea, as a Chief Engineer & Leader of Tactical Communication System team. His research interests include wireless communication system, defence tactical network, IoT, and SDN.



Jong-Man Lee received a B.S. degree, in Department of Electronic Radio Engineering from Kyung hee University, Korea, in 2010, and M.S. degrees in Electrical and Electronic Engineering from Yonsei University, Korea, in 2022. Currently he works at Hanwha Systems, Korea, as a Senior Engineer. His research interests include tactical mobile communication system design in LTE/5G system, and deep learning algorithm related to communication system.



include machine learning and signal processing for wireless communication.

Byungju Lim received the B.S. and Ph.D. degrees in Electrical Engineering from Korea University, Seoul, Korea in 2015 and 2021, respectively. In 2021, he was a Research Professor at Korea University. From 2022 to 2023, He was a Postdoctoral Scholar with the Department of Electrical and Computer Engineering, Tufts University, Medford, MA, USA. Since March 2023, he has been with the Department of Electronic Engineering, Pukyong National University, Busan, South Korea, where he is currently an Assistant Professor. His current research interests



Hyun Park received the B.S. and M.S. degrees in Department of Computer Science and Engineering from Kwangwoon University, Korea, in 2005, and 2007 respectively. Currently he works at Hanwha Systems, Korea, as a Chief Engineer. His research interests include video streaming transmission control technology in IP network, core network technology in LTE/5G system, and tactical network architecture design.



machine learning (ML) for wireless communications, free space optical communications (FSO), and signal processing techniques. He has received awards, including Best Paper Awards in IEEE ICTC 2021, Travel Grant in IEEE GLOBECOM 2020, Bronze Prize in IEEE Seoul Section Student Paper Contest 2020, and Graduate Research Excellence Award at Korea University in 2021. Research.

Ju-Hyung Lee (Member, IEEE) received his Ph.D. at the School of Electronic Engineering at Korea University, Seoul, South Korea, in September 2021, where he received his B.S. degree in 2016. He is currently a Visiting Post-Doctoral Researcher of electrical and computer engineering with the University of Southern California (USC), Los Angeles, CA, USA, and a Research Professor of electrical engineering with Korea University, Seoul, South Korea. His research focus includes optimization and algorithm design for non-terrestrial networks (NTN),



His research interests include cognitive radio systems and power amplifiers, especially in wireless networks, and tactical communications.

Young-Seok Ha received the B.S. degree and M.S. degree in Electronic Engineering from Changwon National University, Changwon, Korea, in 2000 and 2002. He got the Ph.D. course completion in Electrical Electronic and Computer Engineering from Hanyang University, Seoul, Korea, in 2010 After receiving his M.S. degree. He was with Avionics Research & Development Division, Korea Aerospace Industries LTD, from 2002 to 2006. He is currently Principal Researcher at KRIT(Korea Research Institute for Defense Technology Planning and Advancement). His research interests include cognitive radio systems and power amplifiers, especially in wireless networks, and tactical communications.



Young-Jin Han received a B.S. degree, in Information Communication Engineering, from Catholic University of Korea, in 2019. Currently he works for KRIT(Korea Research Institute for Defense Technology Planning and Advancement), as a researcher. His research interests include spectrum efficiency, tactical communications, and mobile communication system.



Jae-Hong Kwon received the B.S. and Ph.D. degrees in Electrical Engineering from Korea University, Seoul, Korea, in 2014 and 2021, respectively. Since 2021, he has been with Samsung Electronics. His research interests include energy efficiency of communication systems, millimeter wave communications, and beamforming techniques.



Young-Chai Ko (Senior Member, IEEE) received the B.Sc. degree in Electrical and Telecommunication Engineering from Hanyang University, Seoul, Korea and the M.S.E.E. and Ph.D. degrees in Electrical Engineering from the University of Minnesota, Minneapolis, MN in 1999 and 2001, respectively. He was with Novatel Wireless as a Research Scientist from January 2001 to March 2001. In March 2001, he joined the Texas Instruments, Inc., wireless center, San Diego, CA, as a Senior Engineer. He is now with the School of Electrical Engineering at Korea University as a professor. His current research interests include the design and evaluations of multi-user cellular systems, MODEM architecture, mmWave and tera Hz wireless systems.